

Design and Manufacturing of Jet to Free Stream Simulator to Experimental Study of Interaction of Oblique Jet in Crossflow

Moslem Ahmadi¹, Mohamad Hojaji^{1*}, Saeed Toolani¹

¹Department of Mechanical Engineering, Najafabad Branch, Islamic Azad University, Najafabad, Iran

*Email of Corresponding Author: Hojaji_m@pmc.iaun.ac.ir

Received: January 20, 2015; Accepted: August 17, 2015

Abstract

The study of interactions of jet into cross flow at different longitudinal and transverse angles of jet was studied. The following components were designed and constructed: a low velocity wind tunnel to produce the uniform flow, a flat plate with a traverse injection system to simulate the jet injection, and a spatial rake to measure the total pressure. The tests were carried out at longitudinal (α) and transverse angles (β) of 60, 75, and 90 degrees and a velocity ratio of 2.5. The free stream and jet stream velocities were set at 20 and 50 meters per second and were constant for all the tests. Results showed that flow field development could be controlled through injecting oblique jets. Decreasing β caused the following results: 1) improved the effects of injection along the mixing direction, 2) increased jet penetration along the plate width direction, and 3) increased the flow wake. In addition, decreasing α led to a slight increase downstream of the nozzle, but failed to produce a significant change in to total pressure coefficient.

Keywords

Wind tunnel design, Injection simulator, Jet in cross flow, Jet (injection) angle

1. Introduction

Injection of jets into free stream has been studied experimentally, analytically, or numerically in the past 50 years [1, 2]. These researches have done in different areas including turbulent flow, drag reduction, heat transfer, and flow mixing. Mixing of jet and cross flow can be observed in many different industrial and environmental problems including boundary layer control, air-fuel mixing in the combustion chamber, film cooling in gas turbine blades, wind mixing with exhaust gases from cooling towers [3, 4], industrial chimneys, water and waste-water duct branching, chemical processes, jets used for mixing unmixable fluids, and exhaust gases flow into the atmosphere in rockets and vertical landing airplanes (where exhaust gases can be used for controlling direction and acceleration of rockets via varying pressure and jet angle parameters). Jet injection into a cross flow (JICF) is the process of discharging fluid from an orifice into the free stream, leading to a complicated flow field. Counter-rotating vortex pairs (CVP), revers flows, horseshoe vortices, etc. are structures in the flow field due to interaction of jet into cross flow (Fig. 1). Understanding physics of the flow and effects of jet injection parameters on the flow field, heat transfer, mixing, drag, etc., are of paramount significance.

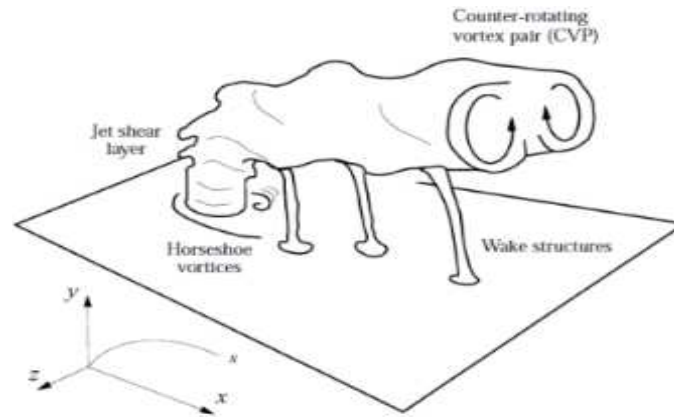


Figure1. Schematic interaction of jet into cross flow

Expected the existence such a complicated flow field, studying the flow field have been attractive to researchers, and much research has been conducted in this discipline in the past 50 years. In particular, heat transfer, control and guidance, mixing, and adjusting specific forces are a certain amount of researches that topic the jet into cross flow studies.

Kamussi, et al. [5] studied the interaction of jet and the free stream at very low Reynolds numbers. The results showed that at low velocity ratios, central line was surrounded by wake vortices. At high velocity ratios, quasi-jet and quasi-wake vortices were observed. If the truth be told, this behavior can be attributed to the jet Reynolds number at different velocity ratios. Reynolds number of the jet plays a essential role in flow instability and emergence of vortices.

Yaw, et al. [6] studied the effects of jet injection angle and the jet exit shape in low jet and free stream Reynolds numbers. They first injected a square vertical jet into the free flow. Also, to better understand the effect of the jet angle, they injected the jet at $\alpha=30$ and $\alpha=60$ degrees. To determine the effect of the nozzle shape exit, they used a circular jet and an elliptical jet at $\alpha=90$ deg at a velocity ratio of 2.5. They observed vortex structures for a square jet were in good agreement with those was observed in other studies. Most findings showed that reduction of jet angle has significant effect on the flow field. Both of circular and non-circular jet cross sections, the flow zone subsequent the jet was wider, and the elliptical jet had a greater width. Among the nozzle exit shapes, the elliptical nozzle exit has the most effects the flow field around the nozzle exit.

In the study by Zaman, et al. [7] on the effect of injecting an oblique jet into the free stream on producing vortices, a jet was injected at $\alpha=20$ deg. in the free stream. Their purpose was observation to the flow field details for different cases of vortex generation due to changing orifice diameter, and boundary layer thickness.

Kickert et al. [8] conducted an inquiry of injecting an oblique jet into the free stream. During this experimental study, they injected a jet under different angles into the free stream, and concluded that discharge angles of greater than $\alpha=40$ degrees, the jet plume developed at downstream.

In the study by Sandraraj et al. [9] on the effects of cross flow jet injection on arbitrary angle for mixing, the jet was injected at longitudinal angles of 45, 60, 90, and 120 degrees. They concluded that the jet central line collapses in 15d for angles fewer than 90 degrees and that in 20d for angles greater than 90 degrees. The increase in jet penetration at high Reynolds numbers improved the mixing of the jet into the free stream; that led to an increase in pressure drop. It's

evident that there is lots of information about the effects of changing the longitudinal angle α has been investigated in previous studies and there is a lack of information about the effects of lateral angle β and its combination with α .

Therefore in the present study the pressure coefficient on the flat plate and the total pressure coefficient of the flow resulting from injecting a circular jet at different longitudinal and transverse angles at constant velocity ratio would be studied.

2. Experimental Setup

The nozzle with exit diameter of 15 mm was mounted on the flat plate injected air into free stream at a constant velocity of 20 m/s. Jet to free stream velocity ratio was assumed to be 2.5. The mechanism for adjusting the jet angle was installed beneath the plate. The study was conducted at α and β angles of 60, 75, and 90 degrees. All distances were made non-dimensional with respect to the jet exit diameter. The inquests were made at the following cross sections: $X/D=-4$, $X/D=-8$, and $x/D=-12$ along the flat plate. The flow field pressure coefficient was measured up to a height of $Z/D=3$ employing a rake. The tests were conducted at 20 C and air was used as the test fluid. A schematic of the flat plate and the jet injection was shown in Figs. 2 and 3.

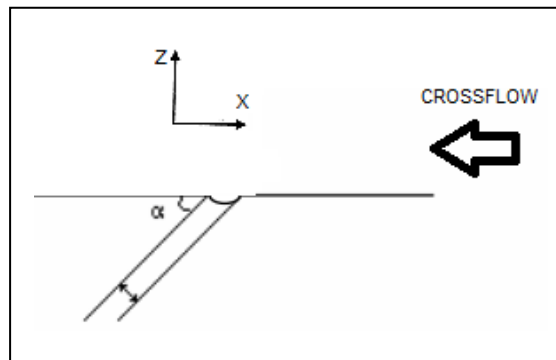


Figure2. Schematic of setting of longitudinal angle (α)

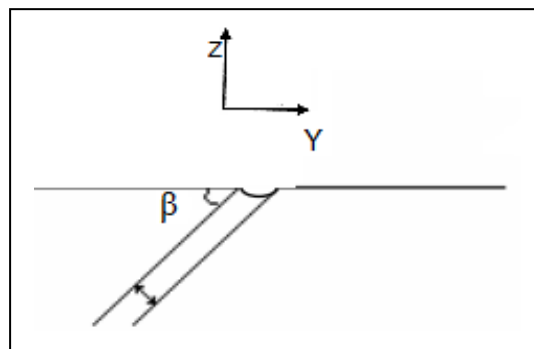


Figure3. Schematic of setting of lateral angle (β)

3. Experimental Apparatus

To do a couple of equipment, a low velocity open circuit wind tunnel was designed and constructed. To provide the maximum free stream velocity (20 m/s) in the test chamber of wind tunnel, powerful fan (3kw) were used. Test chamber dimensions are 0.45 x 1.2 x 0.45 m³ (Fig. 4). A 16-channel rake is used to study pressure variations in the flow field. It comprises 16 steel tubes (1mm in diameter) with a 1 cm spacing (Fig. 5). The flow field pressure variations at

different angles were measured via a 30-channel water manometer (Fig. 6). Static and total pressure probes are used to obtain the corresponding pressures inside the wind tunnel and on the flat plate (Fig. 7).

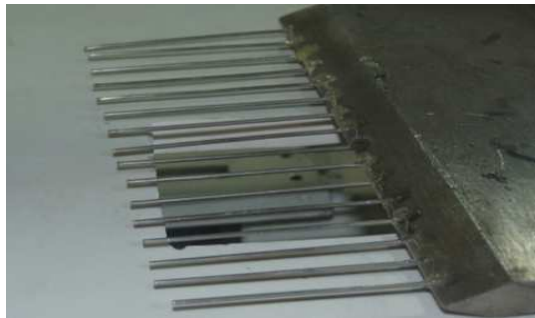


Figure4. Test section

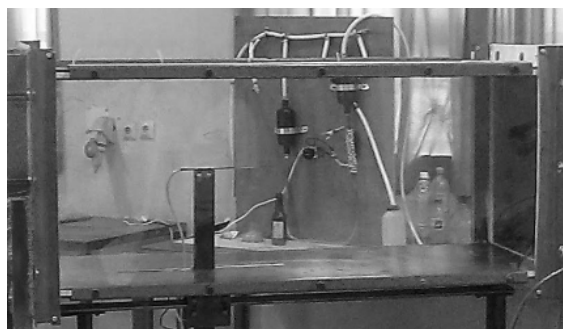


Figure5. Picture of rake



Figure6. Picture of monometer



Figure7. Picture of static Pitot tube

4. Jet Simulator Design and Development

The model is comprised a PVC flat plate (50 x 70 cm²) with a thickness of 10 mm, and a circular nozzle 15 mm in diameter for injecting air at the desired pressure and velocity into the free stream. It had four bases and to provide the possibility of height adjustment and horizontal movement. To measure pressure on plate and around nozzle, 249 pressure orifices (1mm in

diameter) were used on flat plate at proper locations. The front edge of the plate was, through precision machining, adjusted at a particular angle to reduce the disturbances of flow on the plate (Fig. 8). On the plate end, a groove was made for moving the traversing system along the plate. The mechanism for adjusting the jet angle was placed below the plate. This mechanism comprised a jointed level and a ring for holding the nozzle (Fig. 9).

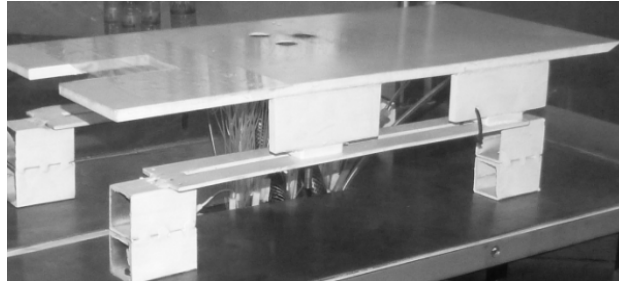


Figure8. Picture of installed flat plate in the test section



Figure9. Mechanism for setting injection angle

5. Governing Equations

Equations 1 and 2 were used to count the surface pressure distribution and total pressure coefficient variation in the jet flow fields. The pressure coefficient and the total pressure coefficient at each point were made no dimensional with respect to the free stream dynamic pressure on the flat plate (Eq. 3).

6. Results and Discussion

In addition to building the jet simulator with variable angles (both longitudinal and transverse), the interaction of an oblique jet interfering with the free stream was also studied. The jet-free stream interaction and the pressure distribution on the flat plate were studied via the C_p pressure coefficient contours. Flow field was studied at three sections through the total pressure coefficient (C_{p_t}). The agreement was observed between the results of this study and those obtained in [10] along the upstream and downstream of jet center line (Fig. 10). The test conditions are presented in Table 1.

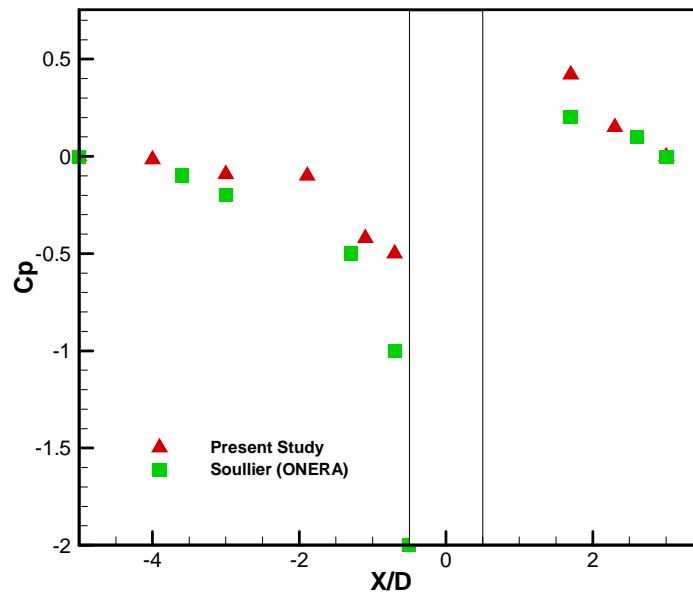


Figure10. Pressure distribution along the center line

Table1. Comparison of flow specifications

N.O	Soullier	Present Study
V_{∞} (m/s)	30	20
D(mm)	120	15
Flat plate	21D×21D	10D×25.6D
Test section	43D×63D	18D×48D
r	2	2.5

6.1 Surface Pressure Distribution under different Jet Angles

The pressure distributions resulting from jet injection into the cross flow at $\alpha=90$ and $\beta=90$ degrees is shown in Fig. 11. It is divided into three regions, namely, upstream, downstream, and in the vicinity of the nozzle. At upstream region, the interaction among the jet and the cross flow created flow field with positive pressure coefficients. In the vicinity of, jet injection led to negative pressure coefficients and jet blockage caused flow acceleration around the nozzle and reduction in the pressure coefficient. At downstream region, pressure coefficient reduced to almost zero due to the increasing distances of the injection point. Fig. 12 shows the surface pressure distribution at $\alpha=90$ and $\beta=75$ degrees. This figure clearly shows the influence of β in deviation. The pressure coefficient at the nozzle upstream is positive, but it reduces dramatically at the downstream. In addition, as shown in the figure, the effect of jet injection persists so far as $Z/D=-5.5$ downstream of the nozzle and $Y/D=3.5$ across the plate. The gradual pressure coefficient reduction in this figure from the upstream to the downstream of the nozzle demonstrated the fact that the wake vortices were increasing. Comparing Figs. 11 and 12 shows that the flow field across the plate developed further as β decreased.

Fig. 13 shows the flow field for $\alpha=75$ and $\beta=90$ degrees. As can be seen, at the upstream of the jet pressure is significantly increased. It can be attributed to the fact that α acts in the opposite direction to the free stream. Around the nozzle, pressure additionally decreases as a result of the flow accelerating in region adjacent to the jet. Finally, in the downstream region, the pressure

drops to almost zero. Comparison of this figure to Fig. 11 shows that decreasing α would increase surface pressure at the upstream and that the effect of the jet diminishes in the downstream region. Fig. 14 depicts surface pressure resulting from jet injection at $\alpha=60$ and $\beta=75$ degrees. The flow field on the flat plate is the result of the jet interacting with the free stream. As it can be observed, the pressure is higher in the vicinity of the nozzle due to the presence of the jet angle. At the jet downstream, pressure drop is observed as the result of jet and free stream interaction. Figure shows that there are no perceptible pressure variations along the jet center line. The reason can be attributed to injection angle. In other word injecting the jet at low angles causes the free stream destroy the jet plume that injected obliquely into the free stream, and the high pressure region in the cross flow is completely destroyed. Fig. 15 shows the surface pressure distribution on the plate in which jet injection angles are $\alpha=75$ and $\beta=60$ degrees. The upstream pressure coefficient is positive, but decreases as we move towards the vicinity of the nozzle. It indicates that wake vortices are being formed, as can be clearly seen at the downstream where the flow field is developed and pressure coefficient reduced. Comparison of Figs. 14 and 15 shows that the wake in latter case is slightly wider and that it is further developed along the Y direction, in spite of the fact that this wake does not seem to be as strong as that seen in the former case.

6.2 Pressure Coefficient Distribution in Flow Field

Figures 16 to 18 show total pressure coefficient at three downstream cross sections. In this case ($\alpha=90$ and $\beta=90$ degrees at first cross section $X/D=-4$). The effects of jet plume are observed until $Z/D=2$. As it can be seen in Fig. 16, greatest pressure coefficient occurs at $Y/D=0$ and $Z/D=2$. As we move downstream, jet plume develops to $Z/D=2.5$. Despite the fact that, pressure coefficient decreases (Figs. 17 and 18).

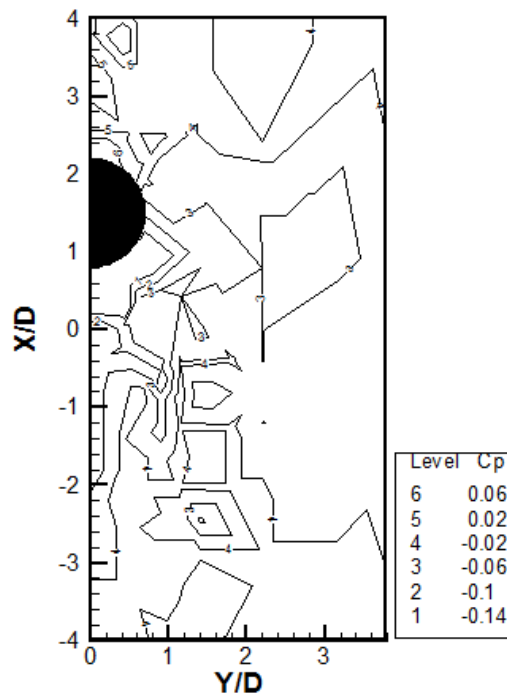


Figure11. Surface distribution around the nozzle exit ($\beta=90$, $\alpha=90$)

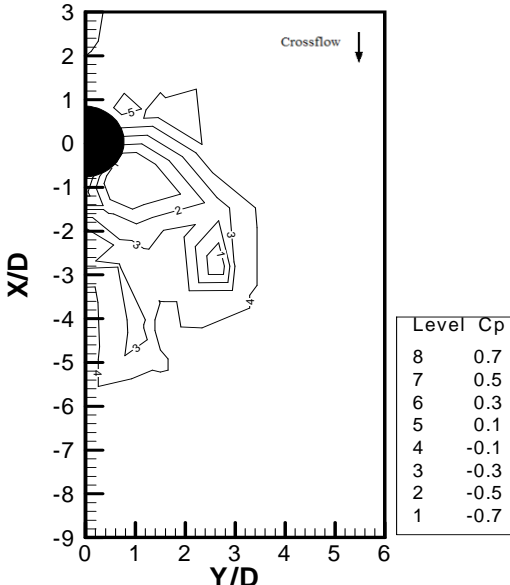


Figure12. Surface distribution around the nozzle exit ($\beta=75, \alpha=90$)

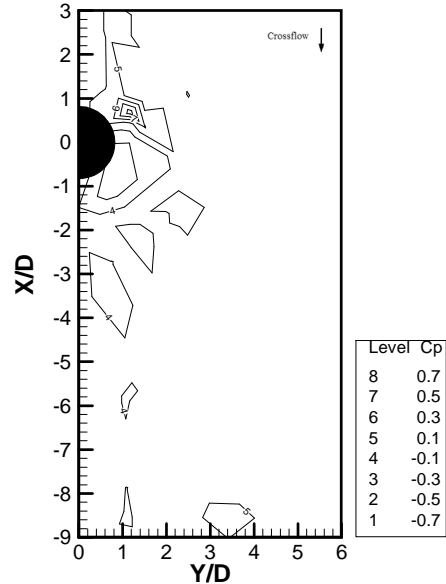


Figure 13: Surface distribution around the nozzle exit ($\beta=90, \alpha=75$)

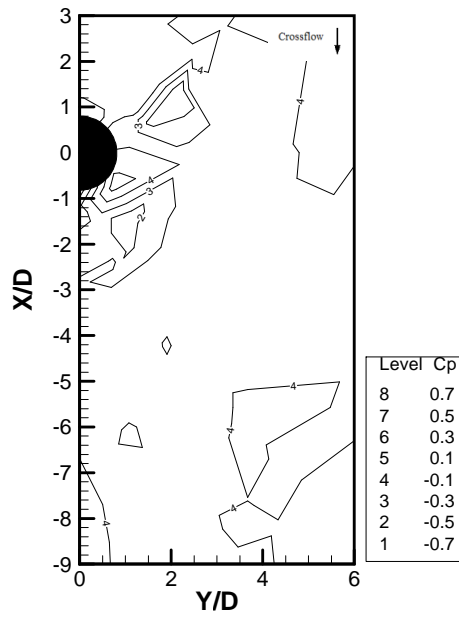


Figure14. Surface distribution around the nozzle exit ($\beta=75, \alpha=60$)

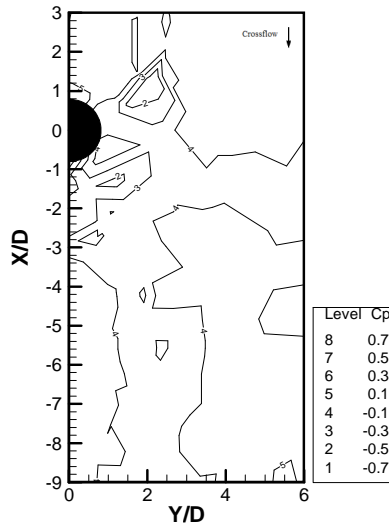


Figure15. Surface distribution around the nozzle exit ($\beta=60, \alpha=75$)

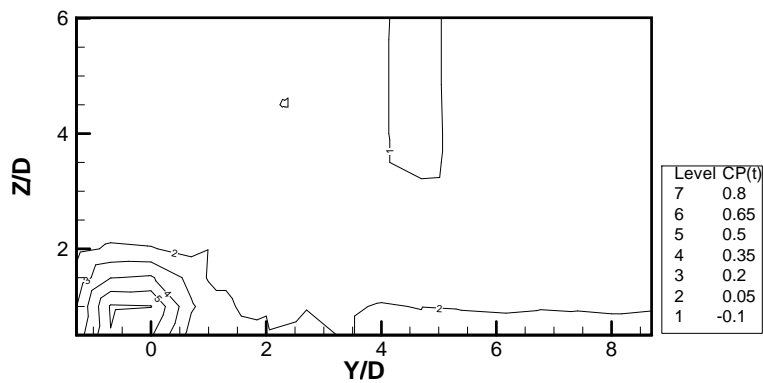


Figure16. Contours of total pressure at cross section $X/D=-4$ ($\beta=90, \alpha=90$)

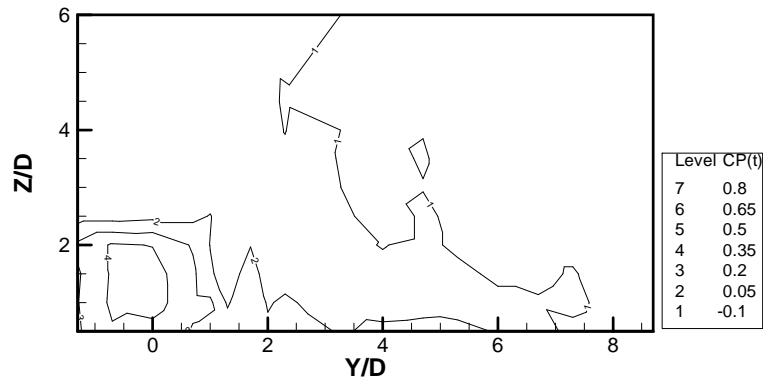


Figure17. Contours of total pressure at cross section X/D=-8 ($\beta=90$, $\alpha=90$)

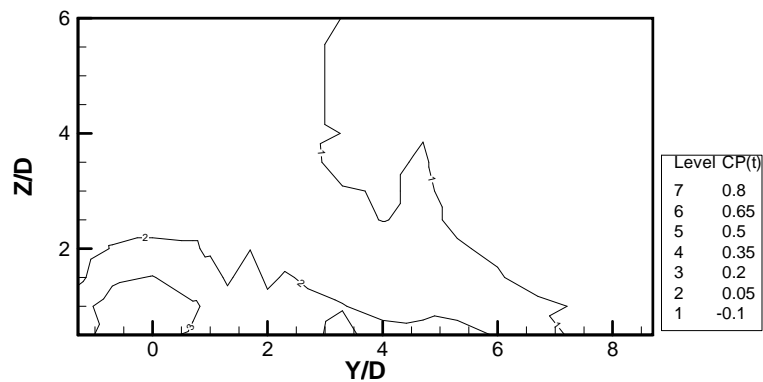


Figure18. Contours of total pressure at cross section X/D=-12 ($\beta=90$, $\alpha=90$)

6.3 Effect of Transverse Angle on Flow Field

Fig. 19 shows the flow field obtained after injecting the jet at $\alpha=90$ and $\beta=75$ degrees and $R=2.5$ at $X/D=-4$ cross section. As observed, maximum pressure coefficient occurs at $Y/D=2.1$ and $Z/D=1.9$. The fact that the maximum pressure coefficient lies in the $Y/D=2.1$ indicates that β indeed affects the jet plume in free stream. Figs. 20 and 21 show total pressure coefficient distribution at $X/D=-8$ and $X/D=-12$. Results show that the total pressure coefficient in the flow field is decreasing. Comparison of the above flow fields shows that although decreasing β leads to better mixing, it reduces jet penetration depth. The total pressure coefficient distribution at several cross sections of second case ($\alpha=90$ and $\beta=60$) are shown in Figs. 22 to 24. Fig. 22 clearly shows the effect of β on the flow field. As can be observed in this figure, the maximum pressure coefficient occurs at $Y/D=2$. As we move downstream, the pressure coefficient decreases, but the location of high pressure region remains constant, maintaining its $2D$ distance from the jet center (Fig. 17). According to Figs. 23 and 24, the pressure coefficient is on the decrease. As we move downstream and as the distance from the nozzle increases, the flow develops further. However, the total pressure coefficient keeps decreasing.

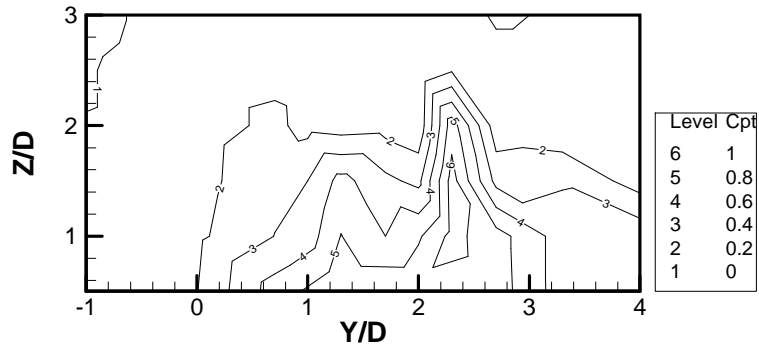


Figure19. Contours of total pressure at cross section $X/D=-4$ ($\beta=75, \alpha=90$)

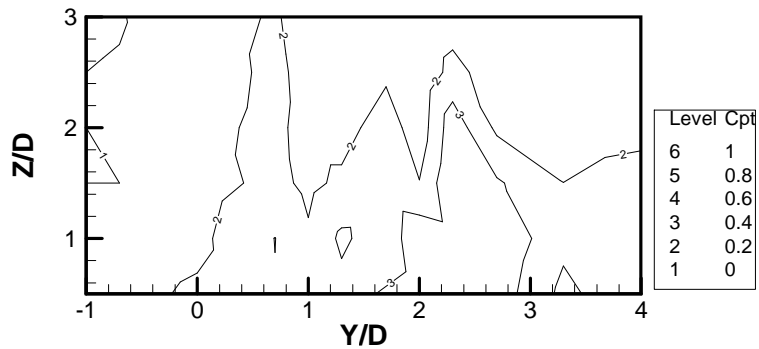


Figure20. Contours of total pressure at cross section $X/D=-8$ ($\beta=75, \alpha=90$)

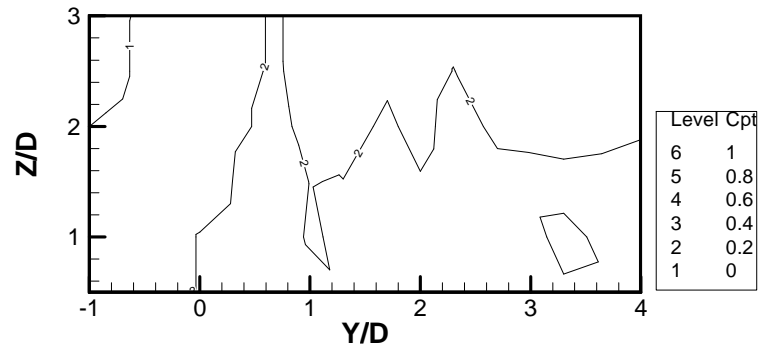


Figure21. Contours of total pressure at cross section $X/D=-12$ ($\beta=75, \alpha=90$)

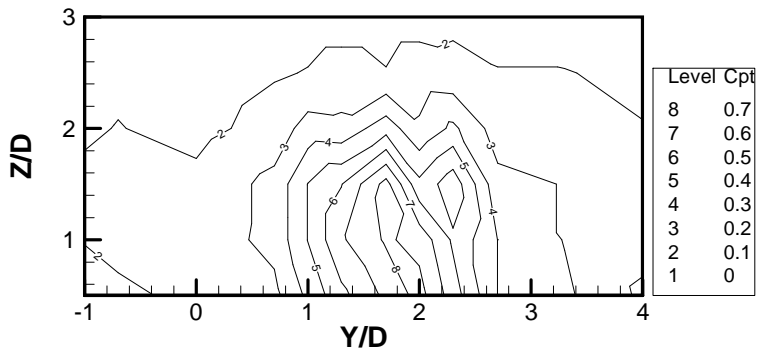


Figure22. Contours of total pressure at cross section $X/D=-4$ ($\beta=60, \alpha=90$)

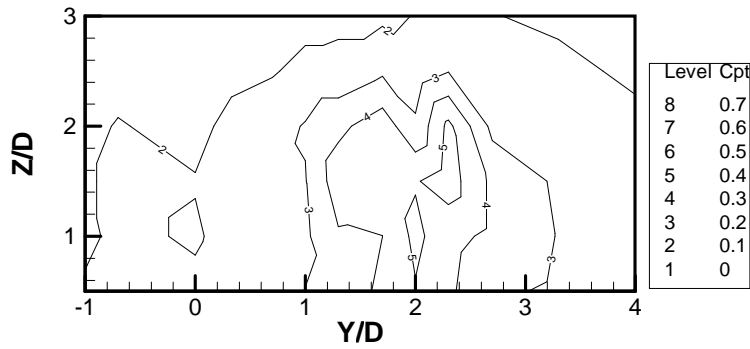


Figure23. Contours of total pressure at cross section X/D=-8 ($\beta=60, \alpha=90$)

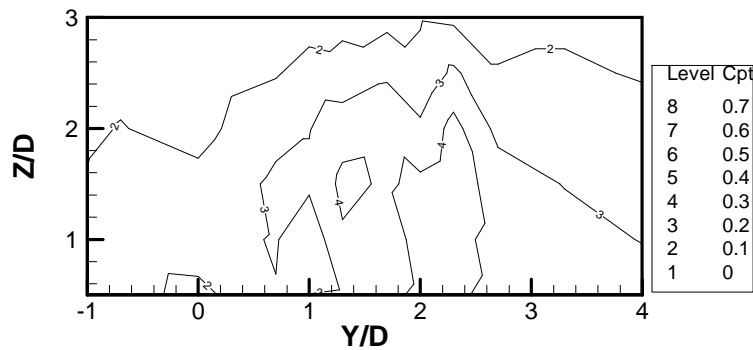


Figure24. Contours of total pressure at cross section X/D=-12($\beta=60, \alpha=90$)

6.4 Effect of Longitudinal Jet Angle Variation on Flow Field

Injecting jet into the free stream at $\alpha=75$ and $\beta=90$ degrees leads to the variations into flow field, as it can be clearly seen in Fig. 25. Results show that influence of jet in this section continues up to $Z/D=3$. Figs. 26 and 27 show the same behavior in the flow field. Despite of the fact total pressure coefficient also decreases in this case. This is indicative of the reduction counter-rotation vortex pair strength. These vortices seem not to have developed at downstream (Figs. 25 to 27).

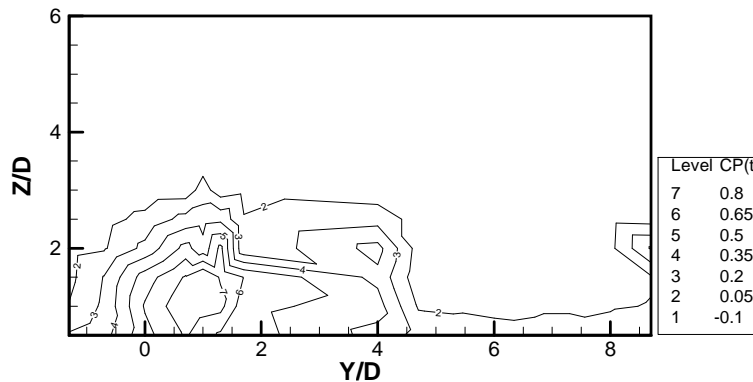


Figure25. Contours of total pressure at cross section X/D=-4($\beta=90, \alpha=75$)

Comparison of above case on Figs. 16, 17, and 18 shows that decreasing α leads to increased jet penetration depth and that flow field extension is also increasing. Fig. 28 shows the total pressure coefficient variations at $X/D=-4$ while jet is injected at $\alpha=60$ and $\beta=90$ degrees. As can be observed, the maximum total pressure coefficient variation occurs within the lower $Y/D=1$ and $Z/D=2$ region, and as we move, the pressure coefficient decreases, and the flow field develops

outwards. This flow development is clearly visible at $X/D=-8$ (Fig. 29) and at $X/D=-12$ (Fig. 30) cross sections. Fig. 28 clearly shows that major flow field variations occur at $Y/D=4$ and $Z/D=3$, and that jet injection effects do not go further than this region.

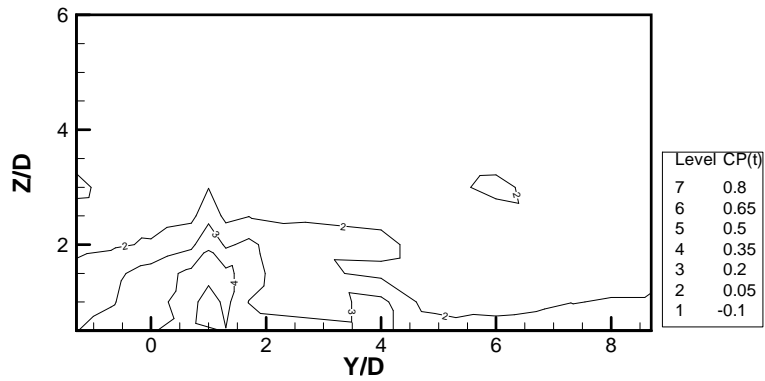


Figure26. Contours of total pressure at cross section $X/D=-8$ ($\beta=90, \alpha=75$)

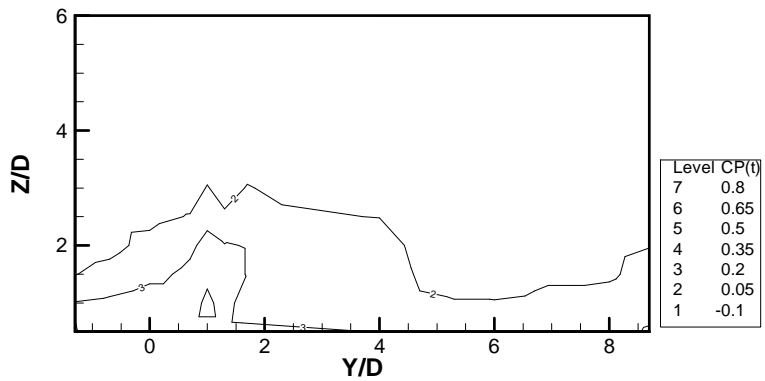


Figure27. Contours of total pressure at cross section $X/D=-12$ ($\beta=90, \alpha=75$)

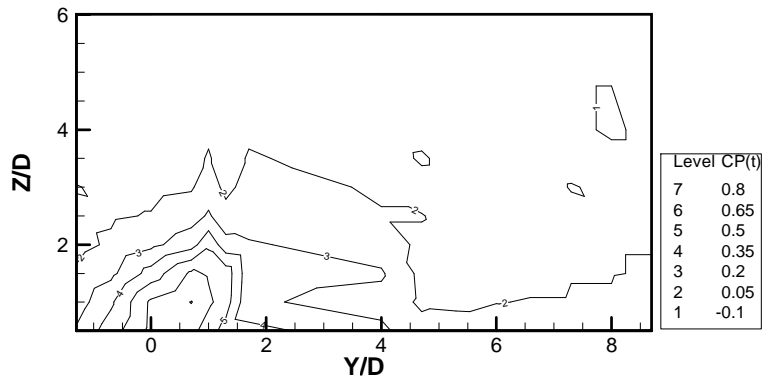


Figure28. Contours of total pressure at cross section $X/D=-4$ ($\beta=90, \alpha=60$)

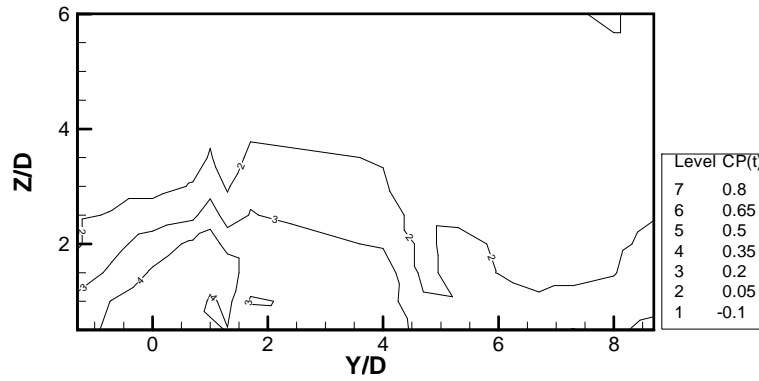


Figure29. Contours of total pressure at cross section $X/D=-8$ ($\beta=90, \alpha=60$)

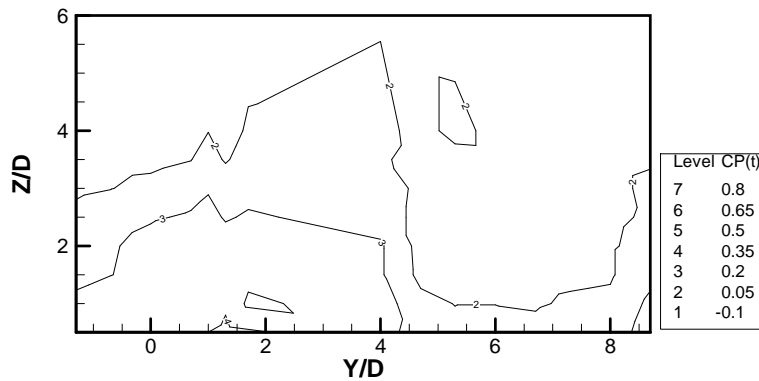


Figure30. Contours of total pressure at cross section $X/D=-12$ ($\beta=90, \alpha=60$)

6.5 Effect of Combination of Longitudinal and Transverse Jet Angle Variations

The resulted flow fields due to jet injection at $\alpha=75$, $\beta=75$, and $X/D=-4$ cross section are shown in Fig. 31. As it can be seen, the effect of jet extends so far as $Y/D=2.5$ and $Z/D=2.1$. The effects of β and α on the flow field are obviously depicted in the form of slight deviation of flow to right (due to β). The maximum total pressure coefficient occurs at $Y/D=0.7$ and $Z/D=1$. As we move downstream, location of this region remains constant. Figs. 32 and 33 show the developed flow field as well as reduction of pressure coefficient. Fig. 34 shows the maximum pressure coefficient in different sections. Maximum pressure coefficient occurs at $\alpha=90$ and $\beta=75$. This shows that proper mixing does not occur for $X/D=0$ to $X/D=-4$ (as compared with other angles), however, at $\alpha=90$ and $\beta=90$, the least effect is created at $X/D=-4$ (as compared with other cases), leading to proper mixing up to this section. Between $X/D=-4$ and $X/D=-8$, the maximum total pressure coefficient decay occurs at $\alpha=90$ and $\beta=75$. Nevertheless, the minimum total pressure coefficient still corresponds to $X/D=-8$ at $\alpha=90$ and $\beta=75$ and $\alpha=90$ and $\beta=90$. At the downstream of the flow, as can be clearly seen, the least total pressure coefficient is obtained for $\alpha=75$ and $\beta=90$ degrees. The diagrams for total pressure coefficient at ($\alpha=90$ and $\beta=60$) and ($\alpha=60$ and $\beta=90$) are similar to each other, showing the jet injection at these angle sets has similar effects on the flow.

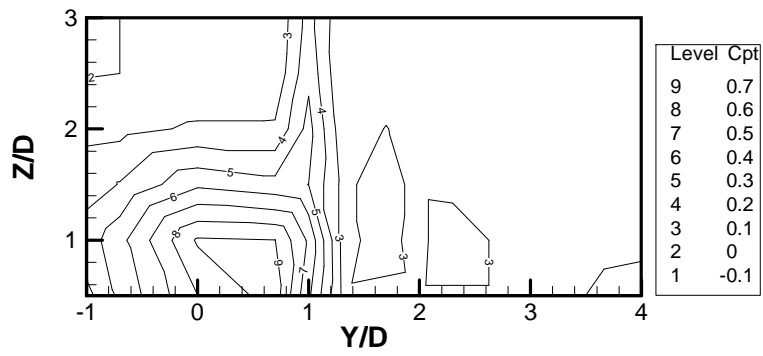


Figure31. Contours of total pressure at cross section $X/D=-4$ ($\beta=75, \alpha=75$)

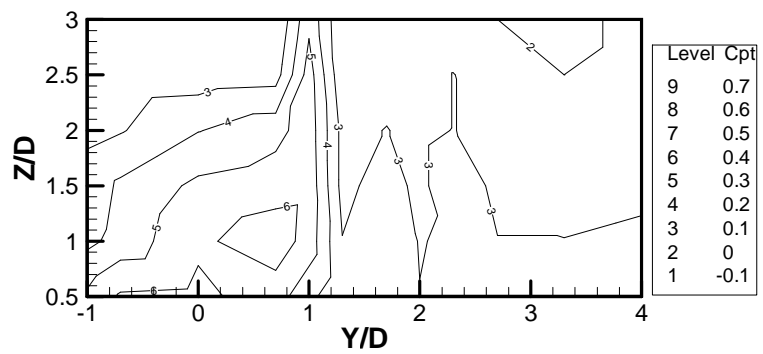


Figure32. Contours of total pressure at cross section $X/D=-8$ ($\beta=75, \alpha=75$)

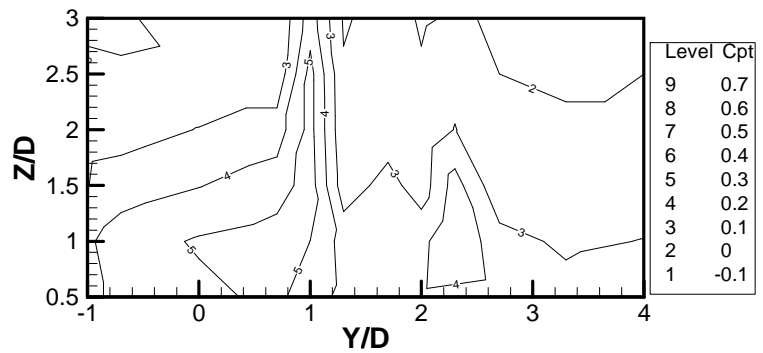
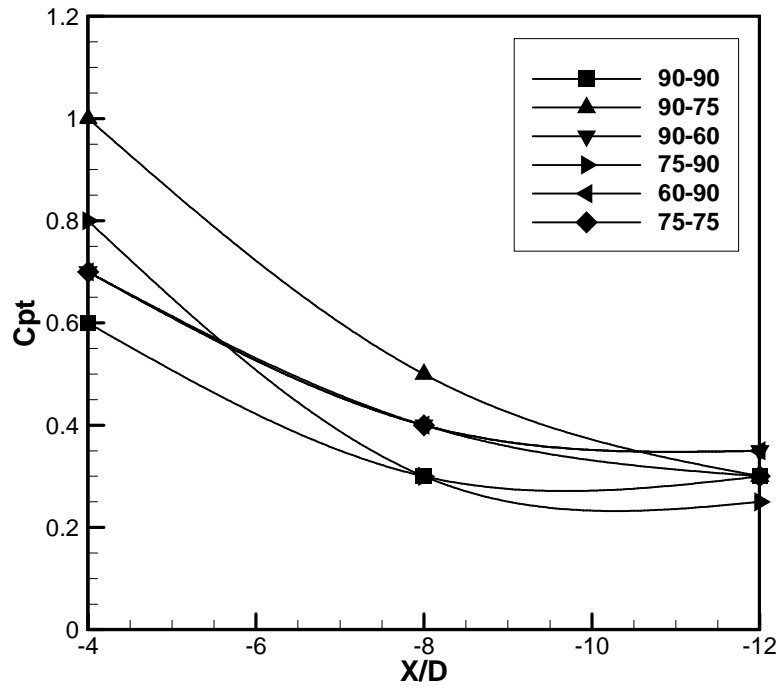


Figure33. Contours of total pressure at cross section $X/D=-12$ ($\beta=75, \alpha=75$)

Figure34. Maximum total pressure distribution at different angles (α - β)

7. Conclusions

The effects of oblique jet and free flow interaction were studied. An in draft subsonic open wind tunnel was used. Jet injection was implemented via a 15 mm nozzle at a velocity ratio of 2.5. Jet velocity was 50 m/s. Effects of jet and free stream interaction as well as pressure distribution on the flat plate were studied. That was made possible by the pressure holes drilled into flat plate. The flow fields were studied through the total pressure coefficient profiles at three sections. They obtained via a 16-channel rake. The results showed that decreasing β at constant α would lead to increase the extension of wakes across the plate and divert flow rightward. Additionally, by decreasing α while keeping β constant lead to decrease pressure coefficient across the plate as well as less developed flow fields. At combined α and β variations, decreasing β further developed the flow field and decreasing α led to the higher pressure in upstream. The flow field after injection showed that increasing α and β led to better mixing of the jet with the free stream. According to this state, the minimum total pressure coefficient was obtained at $\alpha=90$ and $\beta=90$.

8. Nomenclatures

C_p = pressure coefficient

C_{pt} =total pressure coefficient

P =pressure (Pa)

q = dynamic pressure (Pa)

V = velocity (m/s)

α = longitudinal angle

β = transverse angle

ρ = density (kg/m³)

μ = Viscosity (kg/m.s)

9. Subscript

∞	Free stream
j	Jet condition
t	Total condition

10. References

- [1] Margason, R.J., 1993. Fifty Years of Jet in Cross Flow Research, Progress in Energy and Combustion Science, Conference Paper.
- [2] Karagozian, A.R., 2010, Transverse jets and their control, Progress in Energy and Combustion Science, 36(5): 531-553.
- [3] Yusop, N.M., Ali, A.H. and Abdullah, M.Z. 2012. Computational Prediction into Staggered film Cooling Holes on Convex Surface of Turbine Blade, International Communications in Heat and Mass Transfer. 39(9): 1367–1374.
- [4] Curran, E.T. 2001. Scramjet Engines: The First Forty Years, Journal of Propulsion and Power. 17(6):1138-1148.
- [5] Camussi, R., Guj G. and Stella, A. 2002. Experimental Study of A Jet in A Crossflow at Very Low Reynolds Number, Journal of Fluid Mechanic, 454: 113-144.
- [6] Yao, Y., Maidu, M., Yao, J. 2012. Effect of Jet Inclination Angle and Hole Exit Shape on Vortical Flow Structures in Low-Reynolds Number Jet in Cross-Flow. Modelling and Simulation in Engineering, Article ID 632040.
- [7] Zaman, K.B.M.Q., Rigby, D.L. and Heidmann, J.D. 2010. Experimental Study of an Inclined Jet-in-Cross-Flow Interacting With a Vortex Generator. 48th AIAA Aerospace Sciences Meeting Including the New Horizons Forum and Aerospace Exposition.
- [8] Kikkert, G.A. and Davidson, M.J. 2009. A Jet at an Oblique Angle to A Cross-Flow. Journal of Hydro-environment Research. 3(2):69–76.
- [9] Sundararaj, S., Selladurai, V. 2012. The Effects of Arbitrary Injection Angle and Flow Conditions on Venturi-Jet Mixer, Thermal Science. 16(1)207-221.
- [10] Soullier. A. 1972. Distribution of Pressure Around the Jet Orifice, NASA Technical Translation.